Trp-676 Facilitates Nicotinamide Coenzyme Exchange in the Reductive Half-Reaction of Human Cytochrome P450 Reductase: Properties of the Soluble W676H and W676A Mutant Reductases†

Aldo Gutierrez,‡,§,|| Olaf Doehr,⊥ Mark Paine,⊥ C. Roland Wolf,⊥ Nigel S. Scrutton,*,§ and Gordon C. K. Roberts*,‡,§,||

Biological NMR Centre, University of Leicester, Medical Sciences Building, PO Box 138, University Road, Leicester LE1 9HN, U.K., Centre for Mechanisms of Human Toxicity, University of Leicester, Hodgkin Building, PO Box 138, Lancaster Road, Leicester LE1 9HN, U.K., Department of Biochemistry, University of Leicester, University Road, Leicester LE1 7RH, U.K., and Biomedical Research Centre, University of Dundee, Ninewells Hospital and Medical School, Dundee DD1 9SY, U.K.

Received September 11, 2000; Revised Manuscript Received October 20, 2000

ABSTRACT: The kinetics of flavin reduction in two mutant forms of human cytochrome P450 reductase have been studied by stopped-flow spectroscopy with absorption and fluorescence detection. The mutant enzymes were altered at the position of Trp-676, which, by analogy with the structure of rat CPR, is close to the isoalloxazine ring of the enzyme-bound FAD. We show that mutant CPRs in which Trp-676 has been changed to histidine (W676H) and alanine (W676A) can be reduced by NADPH only to the two-electron level in single mixing stopped-flow experiments. The concentration dependence of the rate of hydride transfer indicates that the second, noncatalytic NADPH-binding site present in wild-type CPR is retained in the mutant enzymes. Detailed studies of W676H CPR indicate that further reduction of the enzyme beyond the two electron level is prevented due to the slow release of $NADP^+$ from the active site following the first hydride transfer from NADPH, owing to the stability of a reduced enzyme-$NADP^+$ charge-transfer complex. Reduction to the four-electron level is achieved in a sequential mixing stopped-flow experiment. In this procedure, W676H CPR is reacted first with a stoichiometric amount of NADPH, and then, following a delay of 100 ms, with excess NADPH. The data indicate that occupancy of the noncatalytic coenzyme site also hinders $NADP^+$ release from reduced enzyme. Fluorescence stopped-flow studies of the W676H and wild-type CPR enzymes reveal that the complex signals associated with reduction of wild-type CPR by NADPH are attributable to changes in the environment of residue W676. From these studies, a model is proposed for nicotinamide binding in wild-type CPR. In this model W676 serves as a trigger to release $NADP^+$ from the active site following hydride transfer. In the W676H enzyme, the slow release of $NADP^+$ is a consequence of the combined effects of (i) removing W676 by mutagenesis (thus removing the trigger for displacement) and (ii) the binding of NADPH in the noncatalytic site, thus trapping $NADP^+$ in the catalytic site.

Cytochrome P450 reductase (CPR; EC 1.6.2.4)[1] is a 78 kDa diflavin enzyme located in the endoplasmic reticulum where it donates electrons to a family of cytchrome P450 enzymes (*1*−*5*), which play pivotal roles in the oxidation of a number of endogenous compounds and also catalyze the oxidation of a wide spectrum of drugs and xenobiotics (*6*). CPR contains one molecule of FMN and one of FAD (*7*) and accepts electrons from its reducing substrate NADPH (*8*). It is one of a small family of proteins known to contain both FAD and FMN; other members identified in man include the isoforms of nitric oxide synthase (NOS) (*9*), methionine synthase reductase (MSR) (*10*), and NR1 (*11*). In addition to the P450 enzymes, CPR also donates electrons to other redox acceptors. In vivo, these include cytochrome b_5 (*12*), heme oxygenase (*13*), and the fatty acid elongation system (*14*). CPR can also transfer electrons to a number of drugs including mitomycin c (*15*, *16*), adriamycin (*17*), and the benzotriazine SR4233 (*18*, *19*), and these reactions are believed to have a role in the mechanism of action of these compounds. In vitro, cytochrome *c* and ferricyanide support electron transfer from reduced CPR (*20*, *21*).

CPR comprises three domains that can be separated by limited proteolysis or by genetic methods (*3*, *22*−*25*). The hydrophobic N-terminal domain anchors the enzyme to the

† This work was funded by grants from the MRC and the Lister Institute of Preventive Medicine. N.S.S. is a Lister Institute Research Professor.

* To whom correspondence should be addressed. (G.C.K.R.) Phone: +44 116 252 5533. Fax: +44 116 252 5616. E-mail: gcr@le.ac.uk. (N.S.S.) Phone: +44 116 223 1337. Fax: +44 116 252 3369. E-mail: nss4@le.ac.uk.

‡ Biological NMR Centre.

§ Department of Biochemistry.

|| Centre for Mechanisms of Human Toxicity.

⊥ Biomedical Research Centre.

[1] Abbreviations: CPR, cytochrome P450 reductase; NOS, nitric oxide synthase; MSR, methionine synthase reductase; FRET, fluorescence resonance energy transfer; FNR, ferredoxin-$NADP^+$ reductase; EH_2-$NADP^+$, a form of CPR containing FMN, $FADH_2$ and $NADP^+$; NMN, nicotinamide mononucleotide.

10.1021/bi002135n CCC: $19.00
Published on Web 12/01/2000

endoplasmic reticulum membrane. The FAD and FMN cofactors are contained in distinct structural domains. The C-terminal FAD- and NADPH-binding domain is related to the ferredoxin $NADP^+$ reductase (FNR) family of enzymes (*26*); comparison to the other enzymes of the FNR family reveals a substantial insert in the sequence which folds as an additional domain. The FAD domain is linked by a hinge region to the FMN-domain, which is strikingly similar to the flavodoxins (*27*). The structure of rat liver CPR (lacking the N-terminal membrane anchor) has been determined at 2.6 Å resolution by X-ray crystallography (*28*). The 1.93 Å X-ray crystal (*29*) and NMR solution (*30*) structures of the isolated FMN-binding domain of human CPR have also been determined.

CPR from various sources has been the focus of numerous studies using kinetic (*31*−*34*) and potentiometric methods (*35*, *36*). Our own work has recently focused on the mechanisms of electron transfer in human CPR (*34*). The route of electron transfer is from NADPH to FAD and then to FMN, and the redox potentials of the cofactors are ideally poised for this series of electron-transfer reactions (*36*). We demonstrated recently that electron transfer in human CPR is readily reversible, reflecting its close evolutionary relationship with FNR (*34*). Our kinetic studies have also suggested the presence of a second, noncatalytic NADPH-binding site in human CPR. Occupation of this noncatalytic site by NADPH decreases the rate of hydride transfer from NADPH bound in the catalytic site to the enzyme-bound FAD. The crystal structure of rat CPR indicates that residue W677 is close to the FAD isoalloxazine ring in the catalytic site, partly shielding it from the solvent. The equivalent residue in human CPR is W676, and our previous kinetic studies with the wild-type enzyme have shown that the environment of a tryptophan residue, possibly W676, changes dynamically during the reduction of FAD by NADPH. To understand more fully the role of these changes in the reductive half-reaction of human CPR, and to investigate the interplay between the catalytic and noncatalytic NADPH-binding sites in enzyme reduction, we report here the properties of two mutant forms of CPR in which W676 has been substituted with a histidine or an alanine residue. Our data reveal a role for both W676 and the noncatalytic NADPH-binding site in facilitating nicotinamide exchange during the course of the reductive half-reaction.

EXPERIMENTAL PROCEDURES

Mutagenesis and Protein Purification. Mutagenesis was conducted using the appropriate expression vectors [derivatives of plasmid pET15b (*23*)] encoding human CPR (lacking the N-terminal membrane-anchoring domain) and its NADPH/FAD-binding domain. The cDNA for the human NADPH-cytochrome P450 oxidoreductase was originally derived from a human skin fibroblast cDNA library (*23*). The soluble form of the enzyme (lacking the membrane anchor) was generated by PCR amplification of exons 3−16, followed by subcloning downstream of the 6× histidine linker of the expression vector pET15b (Novagen), generating the expression vector HPET17. Modifications to the 3′ end of the reductase were carried out by PCR. The reductase cDNA contains a *Sma*I restriction enzyme site at nucleotide position 1833, and the vector contains a *Bam*HI site in the multiple cloning site adjacent to the stop codon. A synthetic oligonucleotide (5′-CCG AAT TCG GAT CC T AGC TGT GCA CGT CCA G-3′) containing a *Bam*HI site and the mutant codon (GTG encoding histidine) was used to amplify the region between the natural translation termination and the unique *Sma*I site. The upstream oligonucleotide used was 5′-GTG GCC TTC TCC CGG G AG CAG TCC CAC-3′, which straddles the *Sma*I site. Following digestion with *Sma*I/*Bam*HI, the modified PCR fragment was used to replace the corresponding region in HPET7. A similar strategy was used to prepare constructs encoding W676A CPR and the W676H mutant of the NADPH-FAD-domain of CPR.

Mutant enzymes were purified using the protocol described for wild-type CPR (*37*). The cofactor content of the mutant enzymes was determined by reversed-phase HPLC (*38*) using a Waters ODS2 column (4.6 × 250 nm), which showed that the purified enzymes were stoichiometrically assembled with their constituent cofactors. Protein concentration was determined using the following molar extinction coefficients (M^{-1}-cm^{-1}): CPR 22,000; FAD-domain 11,300 (*34*).

Kinetic measurements. Single turnover kinetic measurements were performed using an Applied Photophysics SX.17MV stopped-flow instrument contained within a customized glovebox (Belle Technology) to maintain anaerobic conditions. Measurements were carried out at 25 °C in 50 mM potassium phosphate buffer, pH 7.0. Protein concentration was 10 μM (reaction cell concentration) unless stated otherwise. All buffers were made oxygen-free by evacuation and extensive bubbling with argon prior to introduction into the glovebox. Prior to stopped-flow studies, all protein samples were treated with potassium hexacyanoferrate (to effect oxidation of the flavins), and excess cyanoferrate was removed by rapid gel filtration (Sephadex G25).

Stopped-flow, multiple wavelength absorption studies were carried out using a photodiode array detector and X-SCAN software (Applied Photophysics Ltd). Spectral deconvolution was using global analysis and numerical integration methods with PROKIN software (Applied Photophysics Ltd). Analysis of single wavelength transients at 450 and 600 nm was as described previously for wild-type CPR (*34*).

Steady-state measurements were performed in a Hewlett-Packard 8452A single-beam diode array spectrophotometer using a 1 cm light path. The desired concentrations of NADPH and horse cytochrome *c* were obtained by making microliter additions from stock solutions to the assay mix. Reactions were performed at 25 °C in 50 mM potassium phosphate buffer, pH 7.0.

RESULTS

In this paper, we have investigated the role of Trp-676 in the kinetic mechanism of human CPR. As inferred from the crystal structure of the rat enzyme (*28*), Trp-676 is positioned over the flavin isoalloxazine ring of the enzyme-bound FAD in human CPR. The role of W676 has been studied by preparing two mutant forms of CPR in which W676 was replaced by histidine (W676H) and alanine (W676A). In our previous studies with human CPR, we demonstrated that the kinetic properties of the isolated FAD-domain mimic closely those of the FAD-domain in the full-length reductase and that the simpler optical spectra of the isolated domain make it easier to measure the kinetics of FAD reduction by NADPH (*34*). We have therefore extended our analysis by incorporating studies of the W676H mutant FAD-domain.

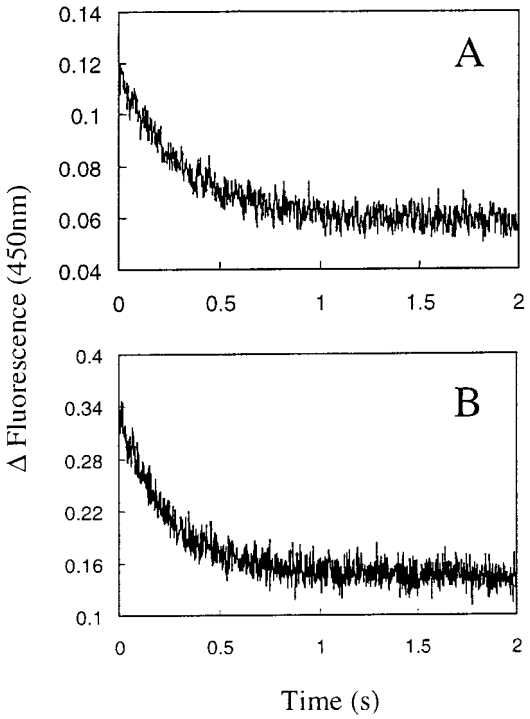

FIGURE 1: Fluorescence transients obtained for the reduction of wild-type (transient A) and W676H (transient B) FAD-domain by NADPH. Conditions: 50 mM potassium phosphate buffer, pH 7.0, 25 °C. [FAD-domain], 10 μM; [NADPH], 200 μM; excitation wavelength, 340 nm; emission wavelength 450 nm. Rates of change of fluorescence emission; wild-type, 3 s^{-1}; W676H, 3.9 s^{-1}.

Stopped-Flow Studies of Flavin Reduction in Isolated W676H FAD-Domain. The kinetics of hydride transfer in W676H FAD-domain were monitored as a reduction in fluorescence emission of NADPH at 450 nm following excitation at 340 nm. Under pseudo-first-order conditions, the rate of hydride transfer (~3 s^{-1}; Figure 1) was found to be similar to the rate of transfer in the wild-type FAD-domain. Hydride transfer can also be followed indirectly as absorption changes accompanying FAD reduction. With the wild-type domain, biphasic transients are observed at 450 nm (ref *34*; Figure 2A); the fast phase (202 s^{-1}) represents the formation of a NADPH-FAD-domain charge-transfer species, and the slower phase (3.7 s^{-1}) represents FAD reduction. Comparable studies with the W676H FAD-domain indicate that the transients observed at 450 nm are also biphasic in this case (Figure 2B). The fast phase (8.8 s^{-1}) represents charge-transfer formation—much slower than in the wild-type—and the slow phase (3.1 s^{-1}) flavin reduction. These assignments are inferred from our studies of wild-type FAD-domain and are substantiated by comparison with photodiode array data (see below) and the kinetics of hydride transfer obtained through fluorescence studies (above) for the W676H FAD-domain.

Notable differences in kinetic behavior between the wild-type and W676 FAD-domains were observed in single wavelength stopped-flow studies performed at 600 nm. As we reported previously for the wild-type FAD-domain, there is a rapid increase in absorption (formation of an NADPH-FAD charge-transfer complex) followed by a slower decrease in absorption (FAD reduction) on mixing this domain with NADPH. The kinetics of these absorption changes are identical to the two phases observed at 450 nm (Figure 3A).

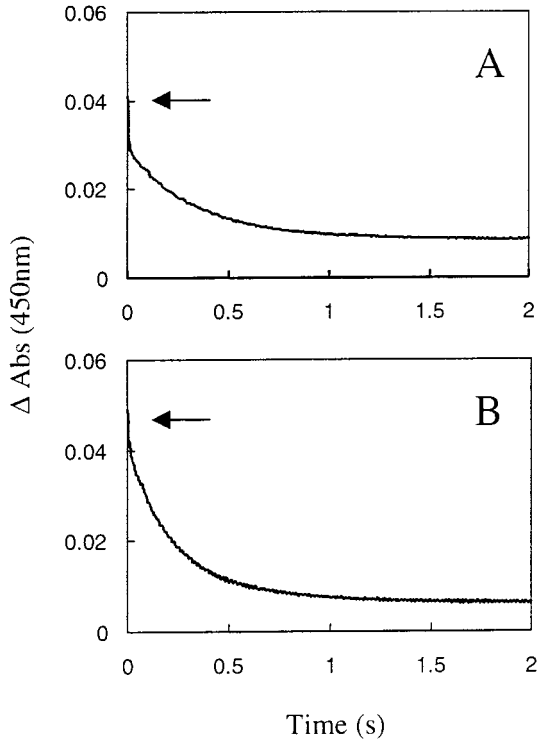

FIGURE 2: Absorption transients obtained for the reduction of wild-type (transient A) and W676H (transient B) FAD-domain by NADPH. Conditions: 50 mM potassium phosphate buffer, pH 7.0, 25 °C. [FAD-domain], 10 μM; [NADPH], 200 μM; absorption detection wavelength 450 nm. Rates of absorption bleaching at 450 nm; wild-type, k_{obs1} (fast phase), 202 s^{-1} and k_{obs2} (slow phase), 3.7 s^{-1}; W676H, k_{obs1} (fast phase), 8.8 s^{-1} and k_{obs2} (slow phase), 3.1 s^{-1}.

In corresponding studies of the W676H FAD-domain, formation of the NADPH-FAD-domain charge-transfer species is clearly seen at 600 nm. The slower rate of formation of this species (8.8 s^{-1}) compared with the wild-type FAD-domain (202 s^{-1}) accounts for the larger signal change with the mutant domain, since the transient absorption change is now well resolved from the dead-time (1.1 ms) of the stopped-flow instrument. However, unlike with the wild-type domain, the optical transient does not return to the baseline absorption level, but remains elevated above the value seen immediately after mixing (Figure 3B). We infer that the residual absorbance at 600 nm observed at the end of the reductive phase is due to the presence of an EH_2-$NADP^+$ charge-transfer species; with the wild-type FAD-domain this charge-transfer species is short-lived and is not observed. With the mutant FAD-domain, the release of $NADP^+$ from the reduced protein is clearly impaired (see also below), whereas with the wild-type domain $NADP^+$ release occurs essentially simultaneously with the reduction process (*34*). The differential absorption changes accompanying the formation of the E-NADPH and EH_2-$NADP^+$ charge-transfer species and flavin reduction in the wild-type and mutant domains are readily seen by multiple wavelength stopped-flow measurements using a photodiode array detector (Figure 3, panels C and D). At 3.8 ms after mixing (the time of acquisition of the first spectrum), the NADPH-FAD charge-transfer species is fully formed with the wild-type FAD-domain, but clearly not with the mutant FAD-domain. With the wild-type FAD-domain, concomitant with flavin reduction, the charge-transfer signature at 600 nm is lost. By

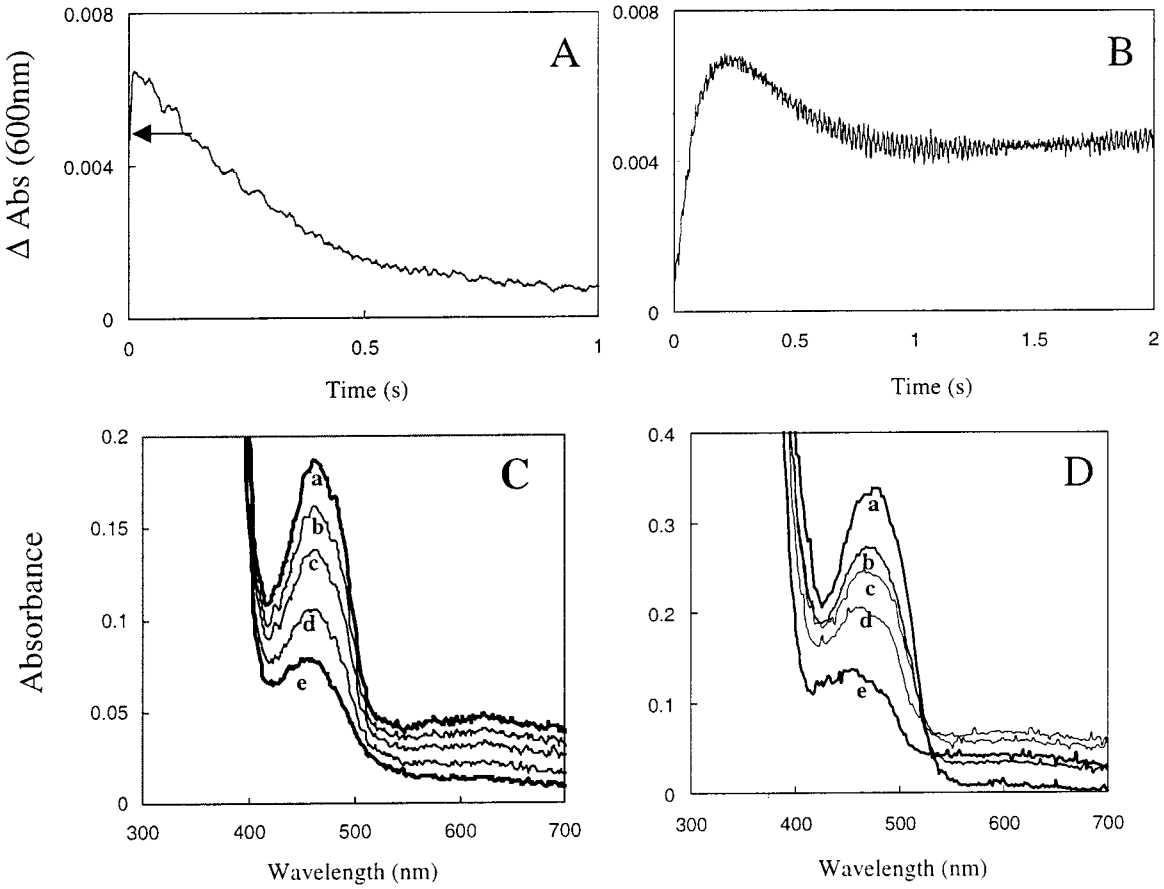

FIGURE 3: Single wavelength (600 nm) and multiple wavelength absorption studies of flavin reduction in wild-type and W676H FAD-domain. Conditions: 50 mM potassium phosphate buffer, pH 7.0, 25 °C. [FAD-domain], 10 μM (single wavelength studies) and 50 μM (multiple wavelength studies); [NADPH], 200 μM. (A) Single wavelength transient at 600 nm obtained for wild-type FAD-domain. The arrow indicates the start of the kinetic transient (some of the absorption increase is lost in the dead-time of the stopped-flow apparatus; see text). (B) Single wavelength transient at 600 nm obtained for W676H FAD-domain. Note, the transient does not return to the initial starting absorption owing to the formation of the EH_2-$NADP^+$ charge-transfer complex. (C) Multiple wavelength data for reduction of wild-type FAD-domain. Note, first spectrum recorded at 3.8 ms (thus significant bleaching at 450 nm has occurred prior to first spectral acquisition) and the charge-transfer signature is developed at 600 nm at 3.8 ms. (D) Multiple wavelength data for reduction of W676H FAD-domain. Note that E-NADPH charge-transfer signature develops prior to FAD reduction and that EH_2-$NADP^+$ charge-transfer signature remains following FAD reduction. For clarity, only selected spectra are shown in panels C and D. In both panels C and D spectrum a to e are recorded at 3.8, 50, 200, 500, and 1000 ms, respectively.

contrast, with the W676H FAD-domain a broad absorption band is observed at long wavelength both prior to flavin reduction (charge-transfer species E-NADPH) and also following flavin reduction (charge-transfer species EH_2-$NADP^+$). Global analyses of the spectral changes occurring with the mutant domain indicate that a two-step model (A $\rightarrow$ B $\rightarrow$ C) is appropriate. The spectra of these species obtained from global analysis of the data are consistent with the presence of oxidized enzyme (species A), an NADPH-FAD-domain charge-transfer species (species B), and an EH_2-$NADP^+$ charge-transfer species (species C).

Stopped-Flow Studies of the W676H CPR. Wild-type and W676H CPR (both lacking the membrane anchor) were used to investigate the mechanism of flavin reduction and to probe for dynamic changes in the environment of W676 during the reduction process. With wild-type CPR, flavin reduction is biphasic [$k_{obs1} = 20\ s^{-1}$, $k_{obs2} = 3.7\ s^{-1}$; Figure 4A (*34*)]. Both phases have been assigned previously to hydride transfer. The first hydride transfer (20 s^{-1}) is faster than the second (3.7 s^{-1}) owing to the very favorable potential difference for the transfer of an electron to the oxidized FMN-domain [$FAD_{sq/red}$ couple, $E_0 = -382$ mV) and $FMN_{ox/sq}$ couple, $E_0 = -66$ mV) (*36*)]. A more detailed discussion of the role of redox potential in driving hydride transfer in CPR has been provided by Gutierrez et al. (*34*). In short, flavin reduction in CPR is reversible, and thus rapid removal of electrons from the FAD-domain (by transfer to the FMN-domain) will increase the observed rate of FAD reduction for the first hydride transfer (*34*). The FMN-domain is less effective in driving the second hydride transfer since the $FAD_{ox/sq}$ and $FMN_{sq/red}$ couples are essentially isopotential in two-electron reduced CPR (*36*). The rate of transfer of the second hydride ion is thus similar to that seen with the isolated FAD-domain.

With the W676H mutant CPR, transients observed at 450 nm were essentially monophasic,[2] and the amplitude of the absorption change was substantially less than that seen with wild-type CPR (Figure 4A). Moreover, the rate of FAD reduction (2.9 s^{-1}) is almost identical with that seen for FAD

[2] There is a small deviation in fits to a single exponential expression at early time points in the transient. This small deviation is likely due to the formation of an NADPH-CPR charge-transfer intermediate prior to hydride transfer. A similar species was identified in stopped-flow studies at 450 nm with the isolated W676H FAD-domain.

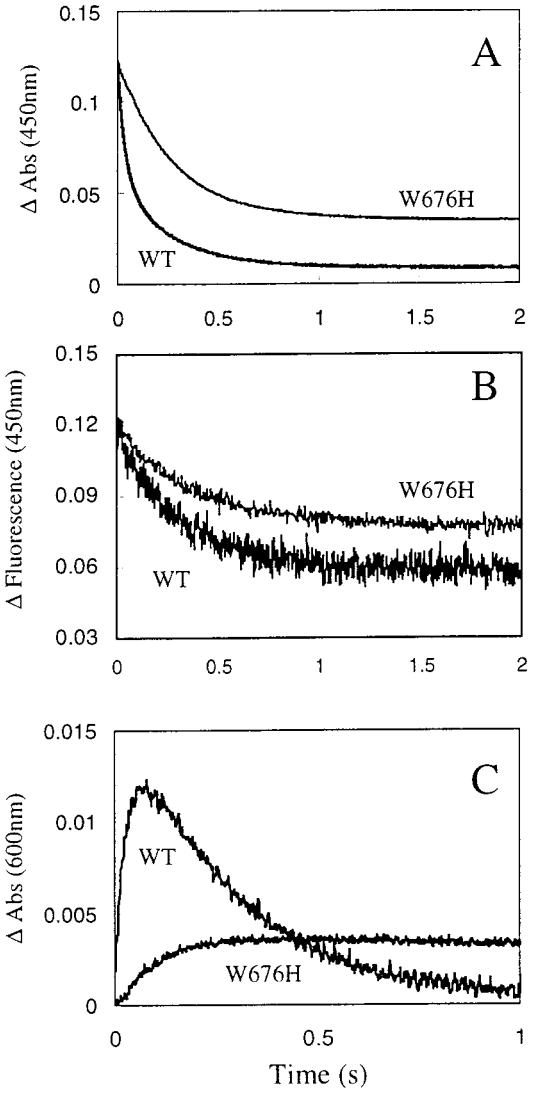

FIGURE 4: Single wavelength absorption and fluorescence transients of flavin reduction and NADPH oxidation by wild-type and W676H CPR enzymes. Conditions: 50 mM potassium phosphate buffer, pH 7.0, 25 °C. [CPR], 10 μM; [NADPH], 200 μM. (A) Absorption transients at 450 nm for W676H CPR and wild-type CPR. W676H CPR (monophasic transient), k_{obs} = 2.9 s^{-1}; wild-type CPR (biphasic transient), k_{obs1} (fast phase) = 20 s^{-1}, k_{obs2} (slow phase) = 3.7 s^{-1}. (B) Fluorescence changes accompanying NADPH oxidation. Excitation wavelength 340 nm, emission wavelength 450 nm. (C) Absorption transients at 600 nm for W676H CPR and wild-type CPR.

reduction in the isolated W676H FAD-domain. In combination, these data suggest that, on the time scale of the stopped-flow experiments, W676H CPR is capable of accepting only a single hydride equivalent from NADPH. Fluorescence studies of hydride transfer also revealed a monophasic reduction process with the mutant W676H CPR, whereas corresponding transients with the wild-type enzyme were clearly biphasic (Figure 4B). Notable differences in kinetic behavior between wild-type and mutant CPR were also observed at 600 nm (Figure 4C). Following the first transfer of a hydride ion to wild-type CPR, a strong absorption at 600 nm is observed which is attributed to the presence of the blue di-semiquinoid species of the enzyme (*34*). The formation of this species occurs at the same rate as the first hydride transfer from NADPH to FAD because internal electron transfer in CPR is rapid (*34*), and it decays with kinetics identical to those describing the second hydride transfer to CPR (Figure 4C). By contrast, in W676H CPR the absorption changes occurring at 600 nm are described by a monophasic increase in absorption (Figure 4C), substantially less in amplitude than that developed for the di-semiquinoid species with wild-type CPR. Importantly, the absorption at 600 nm shows no sign of decreasing even 1 s after mixing, suggesting that a second hydride transfer to W676H CPR does not occur even in the presence of relatively high concentrations of NADPH. By analogy to our observations with the W676H FAD-domain, we attribute the monophasic increase in absorption at 600 nm to the formation of an EH_2-$NADP^+$ charge-transfer species, rather than the development of a di-semiquinoid species. All the kinetic data are consistent with the proposal that $NADP^+$ release is inhibited in the mutant CPR and that only a single hydride anion is transferred in the reductive half-reaction of W676H CPR. The stability of the EH_2-$NADP^+$ charge-transfer species prevents internal electron transfer to the FMN and thus precludes formation of the blue di-semiquinoid species.

Dynamic Changes in the Environment of W676 during Flavin Reduction. Previously, we suggested on the basis of fluorescence studies that W676 in human CPR is conformationally dynamic during flavin reduction (*34*) and that the side chain of this residue would need to move to allow access of the nicotinamide to the FAD isoalloxazine ring. These proposed motions in W676 are consistent with the location of the counterpart residue (W677) in the crystal structure of rat CPR (*28*). We obtained evidence consistent with an NADPH-induced conformational realignment of W676 in wild-type CPR by investigating tryptophan fluorescence and fluorescence energy transfer (FRET) studies during flavin reduction by NADPH. Wild-type CPR displays complex changes in tryptophan emission during the course of flavin reduction with excess NADPH [Figure 5A (*34*)]. We proposed previously that the initial rapid increase in fluorescence is due to NADPH-binding. The subsequent decrease ($\sim$ 20 s^{-1}) has kinetics identical with hydride transfer to form two-electron reduced CPR, and the final slowest kinetic phase ($\sim$3 s^{-1}) has kinetics identical to the transfer of a second hydride ion. The correlation of these fluorescence changes with the absorption data were used previously to argue that $NADP^+$ release itself does not limit the rate of transfer of the second hydride to wild-type CPR (*34*). We now show that in reactions of wild-type CPR with stoichiometric NADPH, the fluorescence emission follows a simpler monophasic increase with time (Figure 5A). This is consistent with our notion that the complex signals seen in reactions with excess NADPH are attributed to the sequential binding and release of, and reduction by, two molecules of NADPH.

Reactions of W676H CPR with excess NADPH reveal that the complex emission signals seen with the wild-type enzyme are absent in the mutant CPR (Figure 5B). Only a relatively small increase in tryptophan emission (about 10% of the total change in emission signal seen with wild-type CPR) is seen in rapid mixing experiments with the mutant CPR, with kinetics similar to those seen in reactions of wild-type CPR with stoichiometric NADPH. As with wild-type enzyme, resonance energy transfer to NADPH can be observed from this tryptophan emission (k_{obs} = 2.6 s^{-1}; Figure 5C) in reactions with W676H CPR. We conclude, therefore, that the complex kinetic changes in tryptophan emission observed

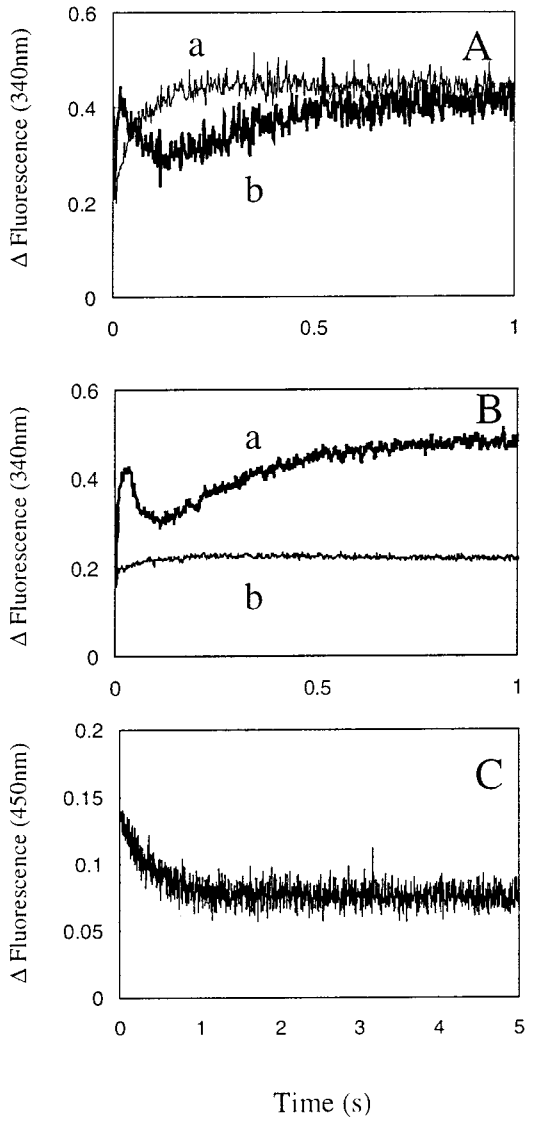

FIGURE 5: Fluorescence kinetic transients and fluorescence energy transfer kinetic transients obtained for the reaction of wild-type and W676H CPR with NADPH. Conditions: 50 mM potassium phosphate buffer, pH 7, 25 °C. Enzyme concentration, 10 μM. (A) Fluorescence emission at 340 nm (excitation 295 nm) for reaction of wild-type CPR with stoichiometric (transient a) and 2-fold excess (transient b) NADPH. (B) Fluorescence emission at 340 nm (excitation 295 nm) for reaction of wild-type (transient a) and W676H (transient b) CPR with 200 μM NADPH (20-fold excess). (C) Fluorescence energy transfer transient for W676H CPR. Excitation = 295 nm; emission = 450 nm.

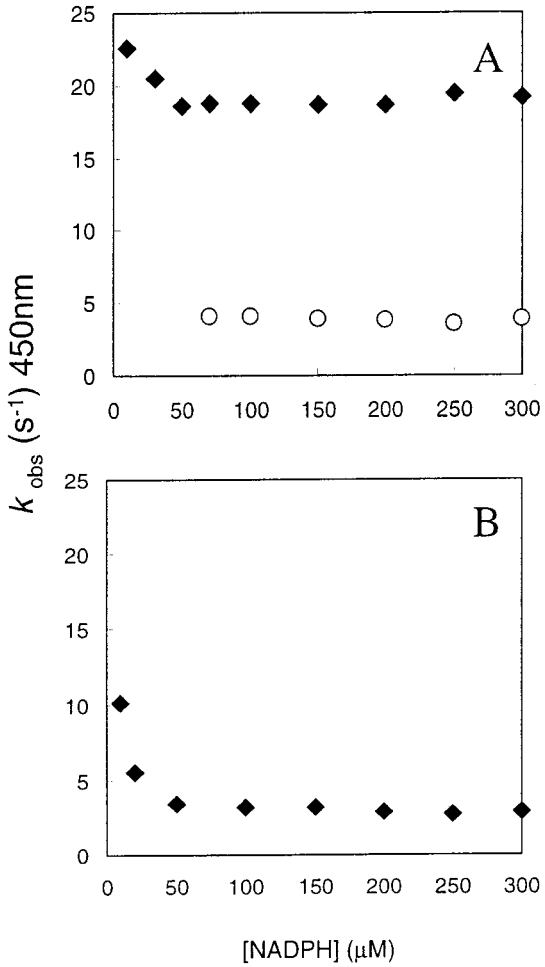

FIGURE 6: NADPH concentration dependence of the rate of flavin reduction (450 nm) for wild-type and W676H CPR. Conditions as in Figure 2. (A) Data for wild-type CPR. (Filled diamonds) First hydride transfer; (open circles) second hydride transfer. (B) W676H CPR (note only one hydride transfer is observed with this mutant CPR).

in reactions of wild-type CPR with excess NADPH are reporting on the induced changes in the environment of Trp-676, and that the very small signals observed with W676H CPR are due to other tryptophan residues in CPR.

Further Evidence for a Second NADPH-Binding Site in CPR. We have earlier provided kinetic evidence suggesting that wild-type CPR contains two binding sites for NADPH (*34*). The rate of FAD reduction in wild-type CPR and the isolated FAD-domain displays an unusual dependence on NADPH concentration. In the pseudo-first-order regime employed in stopped-flow studies of hydride transfer, the flavin reduction rate is independent of NADPH concentration. However, as the NADPH concentration is decreased, the rate of FAD reduction in CPR and the FAD-domain increases. This unusual dependence on NADPH concentration indicates that two molecules of NADPH can bind to the enzyme (*34*). In W676H CPR also, the rate of hydride transfer is accelerated at low NADPH concentration, thus implying that both coenzyme-binding sites are intact in the mutant enzyme (Figure 6). We have used sequential-mixing stopped-flow methods in addition to direct-mixing methods to obtain further evidence for this second site in W676H CPR. Direct mixing of NADPH with W676H CPR under pseudo first-order conditions leads to partial reduction of CPR (Figure 4A), consistent with the transfer of only one hydride ion. However, in experiments in which W676H CPR is reacted for 100 ms with a stoichiometric amount of NADPH prior to the addition of further NADPH (20-fold molar excess over CPR), the mutant CPR is reduced to the same level as is wild-type in a direct mixing experiment (Figure 7). In other words, in this mixing protocol, the W676H CPR is capable of accepting a second hydride equivalent from NADPH.

The data can be interpreted in terms of the following model: direct mixing with excess NADPH leads to occupancy of both the catalytic and noncatalytic NADPH-binding sites in W676H CPR. The release of $NADP^+$ from W676H CPR following hydride transfer is slow and is slowed further by the occupancy of the second, noncatalytic site by

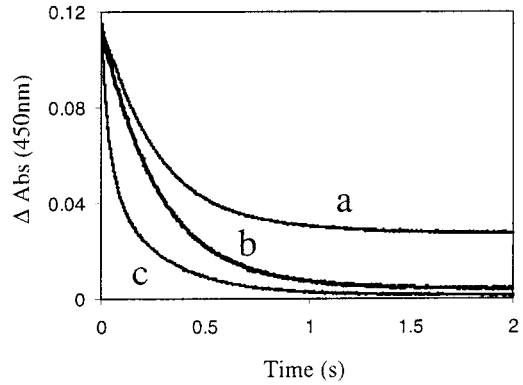

FIGURE 7: Direct mixing and sequential mixing stopped-flow absorption transients (450 nm) for the reaction of W676H CPR with NADPH. Conditions as Figure 2. Transient a, direct mixing of W676H CPR with 200 μM NADPH. Transient b, sequential-mixing transient with W676H CPR. Initial mixing event is 10 μM W676H CPR with 10 μM NADPH; second mixing event involves addition of excess NADPH to a final concentration of 200 μM after 100 ms delay. After 100 ms delay only a small proportion (~10%) of the W676H enzyme is reduced with NADPH (see Figure 4A). Consequently, in the sequential mixing method the amplitude of the transient is approximately equal to that seen with wild-type CPR in a direct mixing experiment. In transient b, therefore, the absorption change reflects the transfer of slightly less than 2 hydride equivalents. As the delay time is increased, the amplitude of the sequential mixing transient observed with W676H CPR is progressively reduced (not shown), owing to the first hydride transfer occurring in the delay period. Transient c, direct mixing of wild-type CPR with 200 μM NADPH.

NADPH. This gives rise to the EH_2-$NADP^+$ charge-transfer complex[3] seen in rapid mixing experiments with W676H CPR; this species persists for >1 s. In the sequential mixing experiments where the enzyme is initially mixed with a stoichiometric amount of NADPH, the noncatalytic coenzyme site is unoccupied. Under these conditions, the 100 ms delay provides sufficient time to poise the enzyme for hydride transfer and to allow the $NADP^+$ to dissociate prior to the binding of excess NADPH. The catalytic site is thus vacated, allowing a second molecule of NADPH to bind and donate a second hydride ion to FAD. At the same time, the NADPH will bind to the noncatalytic site, but without impairing the second hydride transfer, since under the conditions of this experiment the latter does not require $NADP^+$ dissociation.

With wild-type CPR, the release of $NADP^+$ is faster than with the W676H mutant enzyme. The faster release of $NADP^+$ in wild-type CPR is likely triggered by the conformational dynamics of Trp-676 observed in our fluorescence studies (see above). The binding of coenzyme to the second (noncatalytic) NADPH-binding site might facilitate movement of W676, thus effecting the release of the NMN portion of $NADP^+$ from the catalytic site. However, the precise details of the mechanism of nicotinamide coenzyme release and the interplay between the catalytic and noncatalytic sites are the current focus of work in our laboratory. It is worth commenting on the finding that both the wild-type and W676H CPR enzymes display unusual dependence on NADPH concentration in that the rates of hydride transfer are accelerated at low concentration. We surmise that this unusual dependence is in fact due to a slightly different binding geometry of the nicotinamide cofactor in the catalytic site, which is influenced by the presence or absence of NADPH in the noncatalytic site.

Multiple Turnover Studies with Cytochrome c. Figure 8 demonstrates that W676H CPR is functional in its ability to reduce cytochrome *c*. The main difference between the wild-type and mutant CPR is a 3-fold reduction in turnover number on mutating W676 to histidine, although modest changes in the apparent Michaelis constants for both cytochrome *c* and NADPH were also observed. These multiple turnover studies demonstrate that the EH_2-$NADP^+$ charge-transfer complex does not form irreversibly, but that catalysis can proceed to reduce the artificial acceptor cytochrome *c*.

Properties of W676A CPR. We have also studied the effects of removing the large indole side chain of W676 by constructing a W676A mutant of CPR. Single-turnover stopped-flow studies of flavin reduction at 450 nm indicate that hydride transfer is very slow (0.05 s^{-1}) in this mutant (Figure 9A). The extent of reduction is similar to that seen with the W676H CPR, indicating that only a single hydride ion is transferred in the reaction. The transient observed at 600 nm is complex, and the absorption change is in fact larger than one would expect for an EH_2-$NADP^+$ charge-transfer complex (as seen with the W676H CPR; Figure 9B). However, over such long time periods (100 s), disproportionation of the enzyme species is expected, as observed for the wild-type enzyme (*34*), and this will contribute to absorption changes at this wavelength. For this reason, we cannot attribute the absorption changes at 600 nm to individual enzyme species, but the data serve to illustrate that flavin reduction in W676A CPR is in fact highly compromised. The slow rate of flavin reduction is also apparent in multiple turnover reactions of W676A with cytochrome *c* (Figure 9C). The data suggest that, in W676A CPR, the geometry of coenzyme binding is much less optimal for hydride transfer than in either the W676H or wild-type CPR enzymes. This is particularly evident in stopped-flow studies with stoichiometric amounts of NADPH where the inhibition due to binding at the noncatalytic NADPH-binding site is removed (Figure 9D).

DISCUSSION

In the crystal structure of rat CPR, the aromatic ring of W677 shields the isoalloxazine ring of the FAD from the nicotinamide cofactor (*28*), and this residue will clearly need to reposition itself in the E-NADPH complex to enable hydride transfer to the flavin N5. The kinetic studies reported here provide the first evidence bearing on the dynamics of this process. The complex fluorescence transients observed with human CPR, which are lost on mutating W676 to histidine, provide direct evidence for the mobility of W676 in the course of the catalytic cycle of the enzyme. Having demonstrated the mobility of W676 in human CPR, the question arises as to the role of this residue in the reductive half-reaction of CPR.

Our stopped-flow studies with W676H CPR indicate that the rate of hydride transfer to the enzyme-bound FAD is only modestly affected as a result of mutation, while a much larger decrease is observed with W676A CPR; the presence of a large side chain thus appears to facilitate optimal hydride transfer to the flavin. In W676H CPR, following hydride

[3] Strictly this species is an EH_2-$NADP^+$-(NADPH) species.

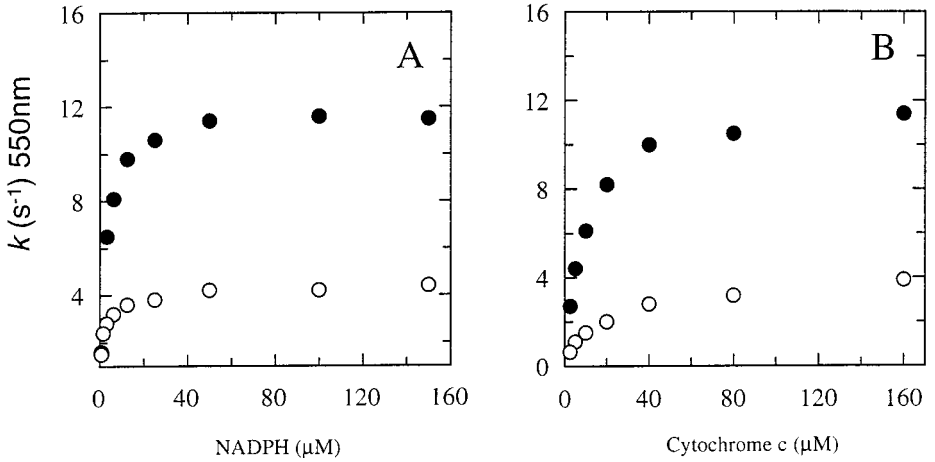

FIGURE 8: Steady-state kinetic analysis of the reaction of wild-type and W676H mutant CPR enzymes with horse cytochrome *c*. Conditions, 50 mM potassium phosphate buffer, pH 7, 25 °C, [CPR], 7 nM. (A) Variation in rate as a function of [NADPH]; [cytochrome *c*], 50 μM. Wild-type CPR (filled circles), apparent $k_{cat} = 12 \pm 0.4$ s^{-1}, apparent $K_m = 3.6 \pm 0.5$ μM. W676H CPR (open circles), apparent $k_{cat} = 4.2 \pm 0.08$ s^{-1}, apparent $K_m = 1.5 \pm 0.2$ μM. (B) Variation in rate as a function of [cytochrome *c*]; [NADPH], 50 μM. Wild-type CPR (closed circles), apparent $k_{cat} = 12 \pm 0.2$ s^{-1}, apparent $K_m = 8.9 \pm 0.5$ μM. W676H CPR (open circles), apparent $k_{cat} = 4.1 \pm 0.08$ s^{-1}, apparent $K_m = 18 \pm 0.2$ μM.

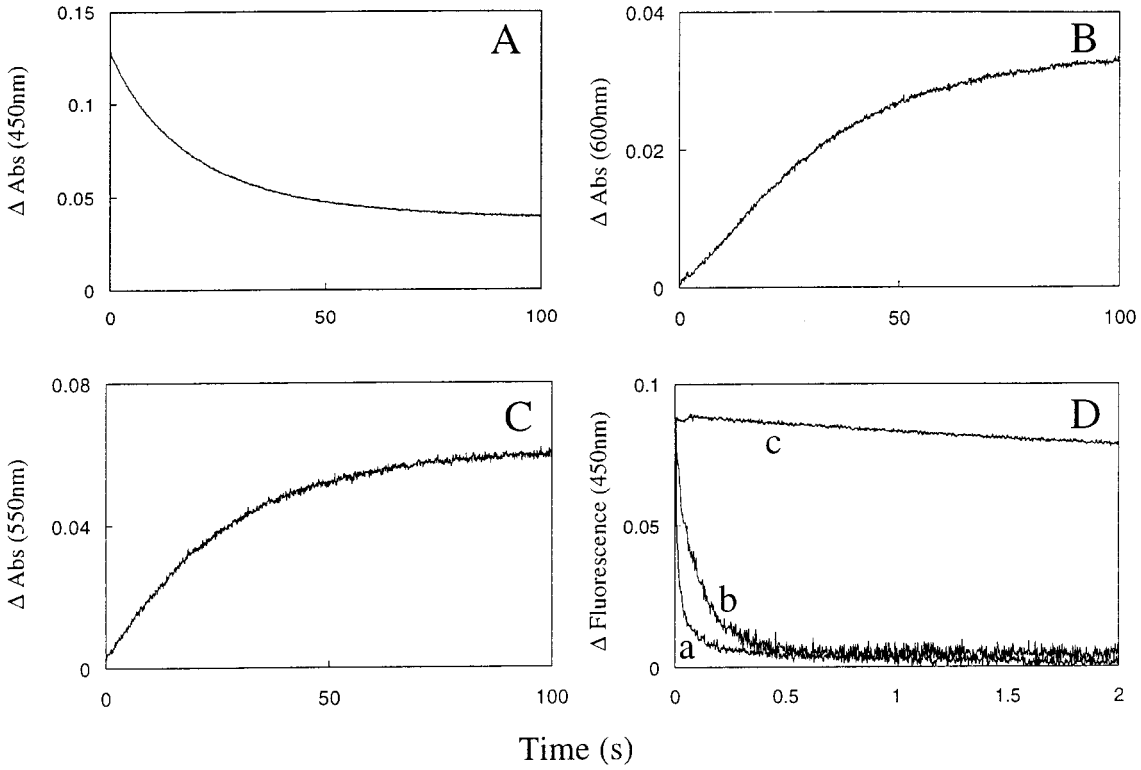

FIGURE 9: Single and multiple turnover stopped-flow transients for the W676A CPR. Conditions as in Figure 2; [Enzyme], 10 μM for single turnover and 0.6 μM for multiple turnover. (A) Absorption transient at 450 nm for flavin reduction in W676A CPR. $k_{obs} = 0.05$ s^{-1}; [NADPH], 200 μM. (B) Kinetic transient observed at 600 nm for the W676H CPR; [NADPH], 200 μM. (C) Multiple turnover stopped-flow transient for the reduction of cytochrome *c* by W676A CPR; [NADPH] 1.2 μM, [cytochrome *c*], 3 μM. (D) Single turnover stopped-flow fluorescence transients of hydride transfer in wild-type, W676H and W676A CPR enzymes with stoichiometric amounts of NADPH. Transient a, wild-type CPR (major phase $k_{obs} = 135$ s^{-1}, minor phase $k_{obs} = 8$ s^{-1}); transient b, W676H CPR ($k_{obs} = 9$ s^{-1}); transient c, W676A CPR ($k_{obs} = 0.2$ s^{-1}).

transfer to the flavin N5, a stable EH_2-$NADP^+$ charge-transfer intermediate is formed. This intermediate is not observed with wild-type CPR, indicating that the release of $NADP^+$ from reduced wild-type enzyme is faster than that from the mutant. These observations have interesting parallels with recent studies of members of the flavodoxin-$NADP^+$ reductase (FNR) family of enzymes, which are structurally related to the FAD-domain of CPR. The physiological direction of hydride transfer in FNR is opposite to that in CPR, but as predicted from the redox potentials of the flavin couples in human CPR (*36*), hydride transfer in the FAD-domain of human CPR is in fact faster in the reverse direction ($FADH_2 \rightarrow NADP^+$) (*34*). In enzymes of the FNR family, the *re*-face of the flavin isoalloxazine ring is shielded by an aromatic amino acid side-chain—tyrosine in FNR, tryptophan in CPR—which appears to prevent productive binding of the

nicotinamide moiety of NADP(H) in spinach FNR (*39*), *Anabaena* FNR (*40*), sulfite reductase (*41*), and rat CPR (26). In pea FNR, it has recently been shown that mutation of this residue to serine stabilizes the E-$NADP^+$ complex (*42*) and allows the nicotinamide ring of the coenzyme to bind productively, close to the isoalloxazine ring (*43*). The available information on members of this family is consistent with the hypothesis (e.g., ref *38*) that the 2′-P-AMP half of NADPH binds tightly to the enzyme, anchoring the cofactor in the active site, while the redox-active NMN portion binds much less tightly and can only bind productively following a movement of the "shielding" aromatic residue. The results presented here provide strong evidence for the existence of similar phenomena in CPR. In the crystal structure of rat CPR the electron density for the NMN part of $NADP^+$ is low and indicates nonproductive mode(s) of binding (*28*). Mutation of W676 to histidine, however, clearly stabilizes the binding of the NMN moiety, at least in the EH_2-$NADP^+$ complex, and leads to the formation of a stable charge-transfer complex, indicative of an increased affinity and of a productive binding mode, with the nicotinamide ring close to the isoalloxazine ring of the FAD.

The high affinity of two-electron-reduced CPR for $NADP^+$ clearly has consequences for subsequent hydride transfer to generate four-electron-reduced enzyme. In stopped-flow studies, the W676H enzyme is "locked" at the two-electron level, since prolonged incubation with excess NADPH does not facilitate further reduction of the enzyme. However, in steady-state assays with horse cytochrome *c*, multiple turnover is seen and the rate of cytochrome *c* reduction is only modestly affected. Clearly, removal of electrons from CPR by cytochrome *c* drives the release of $NADP^+$ from the active site, presumably through the collapse of the EH_2-$NADP^+$ charge-transfer complex. Comparison of the transient kinetic behavior of the wild-type and W676H CPR suggests that W676 in CPR can be likened to a "trigger" that releases $NADP^+$ from the reduced enzyme following hydride transfer.

A complication seen in the reductive half-reaction of human CPR, but not yet reported in studies with FNR, is the existence of a second noncatalytic NADPH-binding site. Evidence for this second site was provided through studies of the unusual NADPH concentration dependence of the rate of flavin reduction, in which hydride transfer is accelerated at low concentrations of cofactor (*34*). The interplay between the noncatalytic site and the residue at position 676 in releasing $NADP^+$ from the active site has been revealed in direct-mixing and sequential-mixing stopped-flow studies of hydride transfer. The sequential-mixing studies indicate that the W676H mutant can be reduced to the four-electron level, but only if sufficient time elapses to allow $NADP^+$ release prior to the binding of excess NADPH. The kinetics of $NADP^+$ release are thus complex and are influenced by NADPH binding to the noncatalytic site. In wild-type enzyme, the release of $NADP^+$ (triggered by W676) is sufficiently fast to prevent the nicotinamide being trapped by the binding of NADPH to the second site. In W676H CPR, the situation is reversed; in a direct mixing experiment, the kinetics of binding to the noncatalytic site are comparatively fast compared with the *intrinsic* rate of release of $NADP^+$ (i.e., when the noncatalytic site is vacant). The result is that $NADP^+$ is trapped in the catalytic site by the presence of NADPH in the noncatalytic site. The physiological relevance and the precise identification of the noncatalytic site are the focus of current work in our laboratory.

REFERENCES

1. Philips, A., and Langdon, R. (1962) *J. Biol. Chem. 237*, 2652−660.
2. Lu, A., Junk, K., and Coon, M. (1969) *J. Biol. Chem. 244*, 3714−21.
3. Porter, T. D. (1991) *Trends Biochem. Sci. 16*, 154−8.
4. Shen, A., and Kasper, C. B. (1993) in *Handbook of Experimental Pharmacology* (Schenkman, J. B., and Grein, H., Eds.) pp 35−59, Springer-Verlag, New York.
5. Strobel, H., Hodgson, A., and Shen, S. (1995) in *Cytochrome P450: Structure, Mechanism and Biochemistry* (Ortiz de Montellano, P., Ed.) pp 225−44, Plenum Press, New York.
6. Ortiz de Montellano, P. (1995), Plenum Press, New York.
7. Iyanagi, T., and Mason, H. S. (1973) *Biochemistry 12*, 2297−307.
8. Vermilion, J. L., Ballou, D. P., Massey, V., and Coon, M. J. (1981) *J. Biol. Chem. 256*, 266−77.
9. Griffith, O. W., and Stuehr, D. J. (1995) *Annual Rev. Physiol. 57*, 707−36.
10. Leclerc, D., Wilson, A., Dumas, R., Gafuik, C., Song, D., Watkins, D., Heng, H. H., Rommens, J. M., Scherer, S. W., Rosenblatt, D. S., and Gravel, R. A. (1998) *Proc. Natl. Acad. Sci. U.S.A. 95*, 3059−64.
11. Paine, M. J., Garner, A. P., Powell, D., Sibbald, J., Sales, M., Pratt, N., Smith, T., Tew, D. G., and Wolf, C. R. (2000) *J. Biol. Chem. 275*, 1471−8.
12. Enoch, H. G., and Strittmatter, P. (1979) *J. Biol. Chem. 254*, 8976−81.
13. Schacter, B. A., Nelson, E. B., Marver, H. S., and Masters, B. S. (1972) *J. Biol. Chem. 247*, 3601−7.
14. Ilan, Z., Ilan, R., and Cinti, D. L. (1981) *J. Biol. Chem. 256*, 10066−72.
15. Keyes, S. R., Fracasso, P. M., Heimbrook, D. C., Rockwell, S., Sligar, S. G., and Sartorelli, A. C. (1984) *Cancer Res. 44*, 5638−43.
16. Bligh, H. F., Bartoszek, A., Robson, C. N., Hickson, I. D., Kasper, C. B., Beggs, J. D., and Wolf, C. R. (1990) *Cancer Res. 50*, 7789−92.
17. Bartoszek, A., and Wolf, C. R. (1992) *Biochem. Pharmacol. 43*, 1449−57.
18. Walton, M. I., Wolf, C. R., and Workman, P. (1992) *Biochem. Pharmacol. 44*, 251−9.
19. Patterson, A. V., Barham, H. M., Chinje, E. C., Adams, G. E., Harris, A. L., and Stratford, I. J. (1995) *Br. J. Cancer 72*, 1144−50.
20. Masters, B. S. S. (1980) in *Enzymatic basis of detoxification* (Jakoby, W., Ed.) pp 183−200, Academic Press, Inc., Orlando, FL.
21. Kurzban, G. P., and Strobel, H. W. (1986) *J. Biol. Chem. 261*, 7824−30.
22. Porter, T. D., and Kasper, C. B. (1986) *Biochemistry 25*, 1682−7.
23. Smith, G. C. M., Tew, D. G., and Wolf, C. R. (1994) *Proc. Natl. Acad. Sci. U.S.A. 91*, 8710−4.
24. Narayanasami, R., Horowitz, P. M., and Masters, B. S. (1995) *Arch. Biochem. Biophys. 316*, 267−74.
25. Hodgson, A. V., and Strobel, H. W. (1996) *Arch. Biochem. Biophys. 325*, 99−106.
26. Karplus, P. A., Daniels, M. J., and Herriott, J. R. (1991) *Science 251*, 60−6.
27. Watenpaugh, D. K., Sieker, L. C., and Jensen, L. H. (1973) *Proc. Natl. Acad. Sci. U.S.A. 70*, 3857−60.
28. Wang, M., Roberts, D. L., Paschke, R., Shea, T. M., Masters, B. S., and Kim, J. J. (1997) *Proc. Natl. Acad. Sci. U.S.A. 94*, 8411−6.
29. Zhao, Q., Modi, S., Smith, G., Paine, M., McDonagh, P. D., Wolf, C. R., Tew, D., Lian, L. Y., Roberts, G. C. K., and Driessen, H. P. (1999) *Protein Sci. 8*, 298−306.

30. Barsukov, I., Modi, S., Lian, L.-Y., Sze, K. H., Paine, M. J. I., Primrose, W. U., Wolf, C. R., and Roberts, G. C. K. (1997) *J. Biomol. NMR 10*, 63−75.
31. Iyanagi, T., Makino, R., and Anan, F. K. (1981) *Biochemistry 20*, 1722−30.
32. Oprian, D. D., and Coon, M. J. (1982) *J. Biol. Chem. 257*, 8935−44.
33. Guengerich, F. P., and Johnson, W. W. (1997) *Biochemistry 36*, 14741−50.
34. Gutierrez, A., Lian, L.-Y., Wolf, C. R., Scrutton, N. S., and Roberts, G. C. K. (2000) *Biochemistry* (in press).
35. Iyanagi, T., Makino, N., and Mason, H. S. (1974) *Biochemistry 13*, 1701−10.
36. Munro, A., Noble, M., Robledo, L., Daff, S., and Chapman, S. (2000) *Biochemistry* (in press).
37. Modi, S., Gilham, D. E., Sutcliffe, M. J., Lian, L.-Y., Primrose, W. U., Wolf, C. R., and Roberts, G. C. K. (1997) *Biochemistry 36*, 4461−70.
38. Klatt, P., Schmidt, K., Werner, E. R., and Mayer, B. (1996) *Methods Enzymol. 268*, 358−65.
39. Bruns, C. M., and Karplus, P. A. (1995) *J. Mol. Biol. 247*, 125−45.
40. Serre, L., Vellieux, F. M., Medina, M., Gomez-Moreno, C., Fontecilla-Camps, J. C., and Frey, M. (1996) *J. Mol. Biol. 263*, 20−39.
41. Gruez, A., Pignol, D., Zeghouf, M., Coves, J., Fontecave, M., Ferrer, J. L., and Fontecilla-Camps, J. C. (2000) *J. Mol. Biol. 299*, 199−212.
42. Piubelli, L., Aliverti, A., Arakaki, A. K., Carrillo, N., Ceccarelli, E. A., Karplus, P. A., and Zanetti, G. (2000) *J. Biol. Chem. 275*, 10472−6.
43. Deng, Z., Aliverti, A., Zanetti, G., Arakaki, A. K., Ottado, J., Orellano, E. G., Calcaterra, N. B., Ceccarelli, E. A., Carrillo, N., and Karplus, P. A. (1999) *Nat. Struct. Biol. 6*, 847−853.

BI002135N